Research Square

Preprints are preliminary reports that have not undergone peer review.
They should not be considered conclusive, used to inform clinical practice,
or referenced by the media as validated information.

Projected Changes in Persistent Heat Events and Cold Waves over Central China Based on a Dynamical–Statistical Downscaling Dataset

Miao Wang[1]
Hubei Climate Center
Ying Shi
shiying@cma.gov.cn

State Key Laboratory of Climate System Prediction and Risk Management/China Meteorological
Siyan Dong
Key Laboratory of Meteorological Medicine and Health
Yuping Yan
National Climate Center, China Meteorological Administration
Xiaocong Liu
Huangpi District Meteorological Bureau
Shulun Gao
School of Statistics, Beijing Normal University

Research Article

Keywords: Central China, Dynamical-statistical downscaling, Regional persistent heat event, Cold wave

Posted Date: November 3rd, 2026

DOI: https://doi.org/10.21203/rs.3.rs-11400039/v1

License: This work is licensed under a Creative Commons Attribution 4.0 International License.
Read Full License

Additional Declarations: No competing interests reported.

Abstract

Persistent heat events and cold waves not only pose severe threats to human health and ecosystems, but are also closely linked to agricultural productivity, transportation systems, and energy supply. Using a high-resolution (6.25 km) dynamical–statistical downscaling dataset, we first evaluated the performance of individual models and their multi-model ensemble (MME)in reproducing the spatial climatology of daily mean, maximum, and minimum temperatures. Changes in persistent heat events and cold waves over Central China were then projected under three Representative Concentration Pathway (RCP) scenarios (RCP2.6, RCP4.5, and RCP8.5) relative to the baseline period (1986–2005). Results show that both individual models and MME can well reproduce the observed spatial patterns, despite a systematic cold bias. Regional persistent heat events are projected to increase markedly in frequency, intensity, duration, and to expand in spatial coverage, particularly under the higher-emission scenarios (RCP4.5 and RCP8.5), with the annual occurrence frequency increasing by approximately 1.5–3.0 events per year under RCP4.5 and by about 3.0–4.0 events per year under RCP8.5. The hot season is projected to start earlier and end later, extending by 1–2 months under RCP4.5 and RCP8.5. Under RCP8.5, the duration of individual heat events in the mid-to-late 21st century is projected to increase by 10–20 days, and nearly half of the region will experience concurrent high temperatures (≥ 35°C). The area from eastern Hubei Province to central Hunan Province is identified as the zone with the highest risk of persistent heat events. In contrast, the annual frequency of cold waves is projected to decline to less than one event per year under all three scenarios in the late 21st century, while extreme minimum temperatures are projected to rise substantially. Cold waves over Central China are projected to evolve toward lower occurrence frequency, a shorter cold-wave season, and shorter individual event duration. Under the high-emission scenario, this reduction in cold-wave frequency extends across most of Central China, and becomes more widespread and pronounced in the late 21st century than in the mid-21st century.

1 Introduction

Since the Industrial Revolution, anthropogenic activities have driven a sustained increase in atmospheric concentrations of greenhouse gases, resulting in unprecedented changes in the global climate system. According to the Sixth Assessment Report (AR6) of the Intergovernmental Panel on Climate Change, the global mean surface temperature during 2011–2020 was approximately 1.1°C higher than that of pre-industrial levels (1850–1900 baseline), and the rate of warming has continued to accelerate (IPCC 2021). Among the most direct and destructive consequences are the pronounced changes in the frequency, intensity, duration, and spatial extent of extreme weather and climate events worldwide (Fischer and Knutti 2015). These changes pose systemic and multifaceted threats to human society, ecosystems, and economic development (Zscheischler et al. 2018). Consequently, understanding and projecting changes in extreme weather and climate events has therefore become a key issue in both climate change science and risk management.

Regional persistent heat events not only pose severe threats to human health and ecosystems, but also strongly affect agricultural productivity, transportation systems, and energy supply (Easterling et al.

2000). In the context of global warming, high-temperature extremes have become more frequent across Asia, Europe, Oceania, and other regions (Masson-Delmotte et al. 2021; Meehl and Tebaldi 2004; Robine et al. 2008). Since the beginning of the 21st century, China has also experienced frequent record-breaking heat events (Ding et al. 2019; Hsu et al. 2020; Lou et al. 2019; Wu et al. 2020). Previous studies have documented a general decrease in extreme cold events and a widespread increase in extreme heat events over most regions of China (Guan et al. 2015; Jiang et al. 2016; Sun et al. 2016; Wang et al. 2017a; Wang et al. 2017b; Yu and Li 2015). Sun et al. (2014) highlighted that rapid urbanization has intensified the warming in China, with the probability of summer extreme heat events increasing more than sixfold during 1955–2013 due to increased anthropogenic activities; even under the RCP4.5 scenario, approximately half of the summers in the next two decades are projected to be hotter than the summer of 2013. Zhang et al. (2017) further projected that, under the RCP2.6, RCP4.5, and RCP8.5 scenarios, the number of high-temperature days across China would increase by 106%, 196%, and 346%, respectively, with marked regional disparities in the magnitude of the increase.

Nevertheless, extreme low-temperature events remain widespread and hazardous. Such events can cause frost damage to crops, while the accompanying freezing rain and snow disasters can severely affect public health, socio-economic systems, and ecosystems (Gasparrini et al. 2015; Hasegawa et al. 2021; Lesk et al. 2016; Ding 2008; Zhou et al. 2022). In recent decades, Europe, North America, and China have experienced multiple record-breaking extreme low-temperature events, such as the extensive low-temperature, freezing rain, and snow disaster in southern China in 2008 (Ding 2008) and Winter Storm Uri that struck North America in February 2021 (James et al. 2021). These events caused substantial loss of life and economic damage (Zhang et al. 2022a; Zhang et al. 2022b). Notably, although the frequency of extreme low-temperature events in China has declined overall since the early 1960s, this decline has gradually slowed or even reversed since the mid-to-late 1990s (Ai et al. 2020; Gong et al. 2012; Qian et al. 2019).

Accurately projecting the evolution of regional extreme temperature events remains a critical challenge in climate change research. Global climate models (GCMs) are the primary tools for projecting future climate change (Han et al. 2019; Li et al. 2023). However, due to their coarse spatial resolution—typically 100–200 km in the Coupled Model Intercomparison Project Phase 6 (CMIP6)—GCMs may not adequately capture fine-scale climatic variations, particularly in regions with complex topography and diverse microclimates (Fuentes-Franco et al. 2014; Sheffield et al. 2013). The limited ability of GCMs to simulate regional precipitation and temperature extremes (Maraun 2016) has motivated the use of regional climate models (RCMs) and statistical downscaling. In recent years, high-resolution RCMs (e.g., 12–25 km simulations conducted under the Coordinated Regional Climate Downscaling Experiment-East Asia, CORDEX-EA) have yielded a series of important findings for China and East Asia (Yu et al. 2015; Yang et al. 2025; Shi et al. 2018; Gao et al. 2018; Niu et al. 2021; Mao et al. 2026). For provincial applications, however, further spatial refinement is needed to capture local variations. A combined approach of dynamical and statistical downscaling offers such refinement for capturing fine-scale structure of climate change, although a finer output alone does not guarantee improved skill in simulating climatic extremes.

Central China, comprising Henan, Hubei, and Hunan provinces, spans the middle and lower reaches of the Yellow River and the middle reaches of the Yangtze River. This region has experienced pronounced climate change in recent decades, with substantial increases in the frequency of both high-temperature days and maximum temperatures over the last 40 years (Liu et al. 2020; Guo et al. 2023). The duration and intensity of extreme heat events both exhibit increasing trends, whereas extreme cold events have generally decreased in duration (Li et al. 2022). In recent years, this region has repeatedly suffered severe climate extremes. For instance, the record-breaking persistent heatwave and drought across the Yangtze River Basin in 2022 placed enormous pressure on agricultural production, water resources, and energy supply in Central China (Hu et al. 2024). In contrast, the severe cold wave in January 2016, popularly called the "boss level" cold wave, brought record-low temperatures together with widespread freezing rain and snowfall to most parts of this region, triggering extensive transportation disruptions and considerable socio-economic losses (Ma and Zhu 2019). These representative cases highlight the region’s high vulnerability to extreme climate events.

However, existing studies for Central China have predominantly focused on simulating and evaluating mean climate state, or have relied on outputs from relatively coarse-resolution models (Wang et al. 2021; Wang et al. 2023). Less attention has been paid to the refined evolution of high-impact climate events (such as regional persistent heat events and cold waves) in high-resolution downscaled projections. To address this gap, the present study employs high resolution (6.25 km) combined dynamical and statistical downscaling simulation datasets over Central China. Based on a systematic evaluation of individual-model performance and multi-model ensemble capabilities in simulating present-day temperatures, we investigate future changes in regional persistent heat events and cold waves under low-, medium-, and high-emission scenarios (RCP2.6, RCP4.5, and RCP8.5, respectively). The analysis focuses on how the frequency, timing, duration, and spatial extent of these two hazards differ among scenarios and future periods, thereby providing climate information relevant to support regional adaptation planning.

2 Data and methods

2.1 Data

The 6.25-km-resolution dataset used in this study was generated using a combined dynamical–statistical downscaling approach, referred to as the high-resolution combined dynamical and statistical downscaling for multivariable (HDM) (Han et al. 2019). The HDM framework consists of two steps: (1) dynamical downscaling using the regional climate model RegCM4.4 (Giorgi et al. 2019) driven by five CMIP5 models at a 25-km resolution over the CORDEX-East Asia Phase II domain; and (2) statistical downscaling through bias correction of the annual cycle and quantile delta mapping calibrated against a high-resolution (6.25 km) dataset from the China Meteorological Administration Land Data Assimilation System (CLDAS). In this study, we used three of the five ensemble members, driven by HadGEM2-ES, MPI-ESM-MR, and NorESM1-M (hereafter referred to as HdR, MdR, and NdR, respectively), under the

RCP2.6, RCP4.5, and RCP8.5 scenarios. The multi-model ensemble mean (MME) denotes the ensemble mean of the three downscaled model members (HdR, MdR, and NdR).

For model evaluation, observational data were obtained from the National Meteorological Information Centre of the China Meteorological Administration. The dataset comprise quality-controlled daily records of meteorological elements (such as daily mean, maximum and minimum temperatures) from 299 meteorological stations across Central China for 2008–2017. The corresponding downscaled simulations (2008–2017) were interpolated onto the observation station location for comparison with observations. To analyze future climate change, the period of 1986–2005 was defined as the baseline period, and projected changes were assessed for the mid-century (2046–2065) and late century (2080–2098) periods.

Model performance was evaluated over two periods. The primary evaluation period (2008–2017) was determined by the temporal coverage of the high-resolution CLDAS dataset, which served as the calibration reference for the statistical downscaling within the HDM framework (Han et al. 2019). As this 10-year time window does not overlap with the baseline period (1986–2005) used for climate change projections, it enables an out-of-sample evaluation of model performance. To further assess the robustness of the model performance over a longer climatological baseline, we also performed an evaluation over the period of 1986–2005. The results for both periods are presented in Table 3 and discussed in section 3.

Table 1
Summary of the datasets used in this study

Data Type	Name	Source	Spatial Resolution	Variables	Period
Model Data	HdR	NCC	0.0625° × 0.0625°	Daily Mean/Maximum/Minimum Temperature (K),	1986–2098
	MdR	NCC			
	NdR	NCC			
Observation Data	Station Observation	NMIC, China	299 stations	Daily Mean/Maximum/Minimum Temperature (°C), Precipitation (mm)	1986–2005 2008–2017

2.2 Definitions of high-impact extreme temperature events

2.2.1 Regional persistent heat events

a. Single-station persistent heat event

Following the meteorological industry standard *Classification of regional high temperature weather process* (QX/T 228—2014), a single-station hot day is defined as a day on which the daily maximum

temperature (Tmax) at a station reaches 35°C or higher. A single-station persistent heat event is identified when single-station hot days persist for at least three consecutive days. The event starts on the first hot day and ends on the last hot day. If one day with Tmax < 35°C occurs, the persistent event is considered interrupted.

b. Regional persistent heat event

A regional hot day is defined as a day on which the daily maximum temperature reaches 35°C or higher at more than 15% of the stations within a given region. A regional persistent heat event is identified when regional hot days persist for at least three consecutive days, during which the spatial coverage of high-temperature weather (daily maximum temperature ≥ 35°C) exceeds 50% of the region on at least one day.

2.2.2 Cold waves

a. Single-station cold-air process

In accordance with the industry standard *Monitoring indices of cold air processes* (QX/T 393—2017) and the national standard *Grade of cold wave* (GB/T 21987—2017), the intensity of a single-station cold-air process, evaluated for periods other than June–August, is determined by the temperature-drop amplitude and the daily minimum temperature at the station. The intensity is classified into three grades: moderate cold air, strong cold air, and cold wave (Table 2). T_{d} denotes the daily minimum temperature, ΔT_{24} is the difference between daily minimum temperature on the previous day and that on the current day, ΔT_{48} is the difference between the maximum daily minimum temperature in the preceding 48 hours and the minimum temperature on the current day, and ΔT_{72} is the difference between the maximum daily minimum temperature in the preceding 72 hours and the minimum temperature on the current day.

b. Regional cold-air process Cold wave

A regional cold-air process is identified when single-station cold air processes of moderate intensity or stronger occur at more than 20% of the monitoring stations for at least two consecutive days. The intensity index I is calculated as:

$$I = (3N_1 + 2N_2 + N_3)/(N_1 + N_2 + N_3)$$

,

where N_1, N_2, and N_3 represent the number of stations experiencing cold waves, strong cold air, and moderate cold air, respectively. A regional cold air process is classified as a regional cold wave when $I \geq 1.95$.

Table 2
Intensity grades for single-station cold air processes.

Intensity grade	Criteria	
	Temperature drop ($\varvec{\Delta}\varvec{T}$)	Daily minimum temperature (T_d)
Moderate cold air	6°C ≤ ΔT_{48} < 8°C	-
Strong cold air	ΔT_{48} ≥ 8°C	-
Cold wave	ΔT_{24} ≥ 8°C or ΔT_{48} ≥ 10°C or ΔT_{72} ≥ 12°C	T_{d} ≤ 4°C

2.2.3 Methods

Future changes in high-impact heat and cold events are examined in terms of several aspects, including occurrence frequency, start and end dates, duration (mean and maximum event length), and spatial coverage. Specifically, the occurrence frequency is quantified as the annual number of heat events or cold waves. For each regional persistent heat wave (cold wave), the start date and end date (i.e., the first and last days on which the event criteria are met) are identified, and the interval between them is defined as the event duration. The first date of a regional persistent heat event (or cold wave) in a given year is defined as the earliest start date, and the last date of such an event is defined as the latest end date.

All high-impact heat and cold events are identified using the bias-corrected HDM dataset rather than the raw RCM outputs.

3 Evaluation of present climate simulation

Figure 1 shows the spatial distributions of the observed and MME-simulated mean, maximum, and minimum temperatures over Central China during 2008–2017, together with the differences between the simulations and observations. The MME reasonably reproduces the observed spatial pattern of the three temperature variables, which are characterized by lower temperatures over the northern and mountainous areas and higher temperatures over the southern and plain areas. Overall, the MME simulation exhibits a systematic cold bias relative to observations. For mean temperature, a weak warm bias (less than 0.1°C) appears in central and northern Henan Province, whereas cold biases prevail over the remaining areas, reaching 0.8–1.0°C in the mountainous areas of western Henan and Hubei provinces and in regions along the Hubei–Hunan border. For maximum temperature, the MME simulates a slight southward displacement of the observed southern high-value center. Weak warm biases (< 0.1°C) are found over central Hunan and northern Henan, while cold biases dominate most of the remaining areas. In particular, the simulated maximum temperatures in the mountains of Hubei and western Henan are 1.3–1.5°C lower than the observations. For minimum temperature, the low-value

center over central Henan shifts slightly eastward, and the high-value centers in eastern Hubei and southern Hunan are displaced westward and slightly southward, respectively. Moderate warm biases (< 0.5°C) are present in parts of central Henan, eastern Hubei, and central Hunan, while cold biases prevail over most of the remaining areas, with larger negative biases ranging from − 0.8 to − 0.5°C across the mountains of western Hubei and western Henan.

Statistical indicators for each model further verify the spatial characteristics described above quantitatively (Table 3). During the main evaluation period (2008–2017), the spatial correlation coefficients (SCCs) for mean and minimum temperatures range from 0.95 to 0.96 for both individual models and MME, with Taylor skill scores (TSs) of 0.90–0.93, indicating that these models reproduce the observed spatial patterns and variability well. For maximum temperature, the SCC (0.88) and TSs (0.77) are lower, whereas the RMSE is higher (0.74–0.76), suggesting slightly weaker performance relative to the other two temperature variables.

For the extended evaluation period (1986–2005), the SCCs remain above 0.85 for all temperature variables across all models. Both values of SCCs and TSs during this period are generally lower than those during 2008–2017. This situation is expected, given that the statistical downscaling transfer functions were calibrated specifically using the 2008–2017 CLDAS data (Han et al. 2019). Nevertheless, the consistently high SCCs (> 0.85) and TSs (> 0.73) during 1986–2005 confirm that the models can well capture the dominant spatial patterns.

Table 3
Spatial correlation coefficient (SCC), standard deviation (SDD), root-mean-square error (RMSE), and Taylor skill score (TS) for annual mean (Tas), maximum (Tasmax), and minimum temperature (Tasmin) of three downscaled models HadGEM2-ES (HdR), MPI-ESM-MR (MdR), and NorESM1-M (NdR) relative to the observations

		2008–2017				1986–2005			
Variables	**Models**	**SCC**	**SDD**	**RMSE**	**TS**	**SCC**	**SDD**	**RMSE**	**TS**
Tas	HdR	0.95	0.97	0.55	0.90	0.93	1.06	1.36	0.86
	MdR	0.95	0.96	0.56	0.90	0.92	0.99	1.09	0.85
	NdR	0.95	0.96	0.56	0.90	0.93	1.01	1.23	0.87
	MME	0.95	0.96	0.56	0.89	0.93	1.02	1.17	0.87
Tasmin	HdR	0.96	0.96	0.60	0.93	0.89	1.07	1.09	0.79
	MdR	0.96	0.95	0.59	0.93	0.85	0.93	1.45	0.73
	NdR	0.96	0.95	0.59	0.93	0.89	1.03	1.06	0.80
	MME	0.96	0.95	0.60	0.93	0.88	1.00	1.12	0.78
Tasmax	HdR	0.88	0.90	0.76	0.77	0.95	1.06	1.10	0.90
	MdR	0.88	0.90	0.75	0.77	0.95	1.04	1.12	0.90
	NdR	0.88	0.90	0.74	0.77	0.95	1.00	1.06	0.90
	MME	0.88	0.90	0.75	0.77	0.95	1.04	1.04	0.90

4 Changes in high-impact heat and cold events

4.1 Regional persistent heat events

Figure 2 presents the projected changes in regional persistent heat events over Central China under the three RCP scenarios, in terms of frequency, seasonal timing, duration and spatial coverage. Under RCP2.6, the annual frequency of events exhibits no significant long-term trend, with anomalies relative to the baseline period (1.7 events per year) mostly ranging between − 0.4 and 1.5 events per year. Under RCP4.5, the frequency increases markedly from the 2040s onwards, generally rising by 1.5–3.0 events per year during the mid-to-late century and exhibiting a steady upward trend. Under RCP8.5, the frequency increases by 3–4 events per year relative to the baseline in most years after 2070 (Fig. 2a). Meanwhile, the hot season tends to begin earlier and end later, expanding the temporal window over which persistent heat event can occur and prolonging the hot season overall. In particular, under RCP4.5 and RCP8.5, the mean earliest start date advances by 1–2 months and the mean latest end date is delayed by 1–1.5 months relative to the baseline values (11 July and 8 August, respectively (Figs. 2b–2c). Consequently, the total length of the hot season may increase by 1–2 months (Fig. 2d). Under

medium- and high-emission scenarios, the mean duration of regional persistent heat events both increases. Under RCP4.5, the duration generally increases by 2–8 days, even exceeding 10 days in certain mid-to-late-century years. Under RCP8.5, it increases by 10–20 days during most mid-to-late-century years and reaches 20–30 days in some cases. These changes indicate more persistent heat events, with event durations potentially extending by 2–4 weeks relative to the baseline (10.4 days) (Fig. 2d). Furthermore, the average spatial coverage exposed to high temperatures (≥ 35°C) expands under all scenarios. The largest expansion appears under RCP8.5, where the coverage increases by 5–10 percentage points (pp) relative to the baseline (33.4%) during the mid-to-late century and exceeds 10 pp in certain years, suggesting that nearly half of the study region may experience high temperatures simultaneously (Fig. 2e). In summary, changes in regional persistent heat events under the low-emission scenario are relatively moderate, although notable interannual variability and locally extreme years still occur. Under medium- and high-emission scenarios, by contrast, the frequency, duration and spatial coverage of high-temperature events all increase markedly.

Relative to the 1986–2005 baseline, single-station persistent heat events over Central China are projected to intensify markedly in the future, particularly under medium- and high-emission scenarios. These changes are evidenced by more frequent events, higher extreme maximum temperatures, and longer mean and maximum event durations (Fig. 3). Specifically, in the mid-21st century, the frequency of single-station events increases slightly under RCP2.6, increasing by less than 0.5 events in most areas and even decreasing slightly (− 0.1 to 0.0 events) in parts of central Hunan. Under RCP4.5, the frequency increases notably, reaching 1.5 to 2.5 events across most areas, with a maximum exceeding 3.0 events. Under RCP8.5, the frequency increase becomes substantial, with most areas projected to experience 2.5–3.0 additional events (Figs. 3a–3c). Extreme maximum temperatures during events increase by less than 0.5°C across most regions under RCP2.6, except in some northern areas where warming of 0.3–1.5°C is projected. Negative anomalies (− 0.3 to 0.0°C) appear in parts of Henan, southern Hubei, and Hunan. Under RCP4.5, extreme maximum temperatures increase by 0.5–1.6°C across most areas, whereas under RCP8.5, the increase reaches 1.6–2.1°C in central and northern parts of the region and 2.1–2.6°C in most of southern Hunan (Figs. 3d–3f). Mean event duration extends by 0.0–0.7 days in most areas under RCP2.6, with slight shortening in some parts of Hubei and western Hunan. The spatial patterns under RCP4.5 are similar to those under RCP8.5, with decreased duration in western Hubei and northwestern Hunan, whereas most other regions show increases of 0.7–1.7 days, exceeding 1.7 days in some areas (Figs. 3g–3i). The maximum duration increases by 0.0–2.0 days in most areas under RCP2.6, although slight decreases occur in parts of western Hubei and northwestern Hunan. Under RCP4.5, maximum duration lengthens evidently, with most regions increasing by 2.0–4.0 days. Under RCP8.5, the lengthening of maximum duration is similar to those under RCP4.5, but relatively smaller in parts of central and southern Hunan (Figs. 3j–3l).

In the late 21st century, the area showing reduced frequency under the RCP2.6 scenario is slightly larger than that in mid-century. Under RCP4.5, the area with increased frequency expands further relative to mid-century, with most regions experiencing an additional 2.4–4.1 events. Under RCP8.5, the increase becomes pronounced, exceeding 4.9 events across most areas and reaching more than 5.7 events in

some regions, suggesting a high frequency of regional persistent heat events (Figs. 4a–4c). With respect to the extreme maximum temperature in the late 21st century, the values under RCP2.6 decrease relative to the mid-century, particularly in parts of Hubei. Under RCP4.5, the increases in extreme maximum temperature generally reach 2.3–3.0°C, whereas under RCP8.5 they exceed 3.8°C across most of the region and surpass 4.5°C in several local areas (Figs. 4d–4f). Regarding the average duration of persistent heat events in the late 21st century, the values in Hubei and western Hunan reduces under RCP2.6, although the affected area expands relative to that at mid-century. Under RCP4.5, the average duration increases in most areas by 1.2–1.7 days and exceeds 1.7 days in some areas. Under RCP8.5, the average duration increases by more than 2.3 days, reaching 2.9–3.5 days in most central and eastern parts, indicating a substantial prolonging of individual heat events (Figs. 4g–4i). As for the maximum duration in the late 21st century, the area with decreased values expands in parts of western Hubei and northern Hunan under RCP2.6, whereas increases of 4.9–7.3 days appear in some eastern areas under RCP4.5. Under RCP8.5, the maximum duration is projected to increase across most of the region, with the increase generally ranging from 9.8 to 12.2 days. Notably, this increase in maximum duration exceeds 14.6 days in eastern Hubei and central-southern Hunan, indicating that individual extreme heat events may be extended by more than two weeks (Figs. 4j–4l).

Analysis of the four key indicators reveals that the central and eastern parts of Central China (including southern Henan, most of Hubei, central-eastern Hunan) exhibit the most pronounced increases and correspondingly the highest risks of high temperatures under all of the scenarios. Therefore, this area is the core region for the intensification of regional persistent heat events. In contrast, changes are relatively moderate in the western mountainous areas (including northwestern Hunan and western Hubei), reflecting the impact of latitude and topography on regional persistent heat events. Under RCP8.5, in the late century, spatial heterogeneity in all four indicators decreases markedly, with uniformly large changes across the entire region. This suggests that, without emission controls, the entire Central China will face severe extreme heat risk without exception. The magnitudes of changes in most indicators in the late century far exceed those at mid-century, indicating that heat risk increases with time and highlighting the importance of long-term adaptation strategies. The increases in both frequency and average duration suggest more frequent and longer-lasting regional persistent heat events. The pronounced increases in extreme maximum temperature and maximum duration in the late century under RCP8.5 collectively reveal that regional persistent heat events will become increasingly intense and extreme in the future.

4.2 Cold Waves

Table 4 summarizes the annual mean frequency, earliest start date, latest end date, and duration of cold waves over Central China during the baseline period and for three future emission scenarios in the mid- and late 21st century. Except a slight increase under RCP4.5 at mid-century, cold wave frequency decreases under all scenarios and periods, with a greater decline in the late 21st century relative to the mid-century. The most pronounced reduction occurs under RCP8.5, suggesting that cold waves over Central China may become less frequent in the future. The earliest start date advances relative to the

baseline period under all scenarios, although the magnitude of change varies across scenarios and periods. Relative to the baseline-period mean of January 19, the earliest start date advances to January 16 at mid-century and to January 14 in the late 21st century under RCP2.6. Under RCP4.5, it advances to January 15 at mid-century and, more markedly, to January 3 in the late century. Under RCP8.5, it advances to January 17 at mid-century and to January 9 in the late century. The latest end date also advances under all future scenarios. Relative to the baseline-mean of January 22, the greatest advances occur under RCP4.5 and RCP8.5 in the late century, while the other scenario-period combinations show smaller advances of 2–5 days. The mean duration of cold waves is 1.96 days during the baseline period. Relative to this value, the duration slightly increases only under RCP4.5 at mid-century and decreases in other future periods, with the largest decline projected under RCP8.5 in the late century.

Overall, cold-wave frequency over Central China is projected to decrease in the future. Both the earliest start and latest end dates tend to shift earlier, and the duration of individual cold waves also exhibits an overall decreasing trend.

Table 4
Statistical values of cold wave frequency, mean earliest start date, mean latest end date, and mean duration over Central China during the baseline period and under the three emission scenarios at mid- and late century

		Annual frequency (events)	Mean earliest start date	Mean latest end date	Mean duration (days)
1986–2005		1.08 (0.70–1.40)	01/19 (01/07–02/05)	01/22 (01/10–02/08)	1.96 (1.62–2.25)
RCP2.6	Mid-century	1.05 (0.60–1.55)	01/16 (01/13–01/18)	01/19 (01/16–01/21)	1.89 (1.48–2.23)
	Late century	0.91 (0.53–1.47)	01/14 (01/08–01/20)	01/17 (01/11–01/23)	1.78 (1.00–2.44)
RCP4.5	Mid-century	1.18 (0.80–1.40)	01/15 (01/03–01/29)	01/18 (01/06–02/01)	2.03 (1.82–2.15)
	Late century	0.91 (0.58–1.32)	01/03 (12/29–01/07)	01/06 (12/31–01/10)	1.69 (1.42–1.96)
RCP8.5	Mid-century	0.92 (0.80–1.10)	01/17 (01/10–01/27)	01/19 (01/13–01/30)	1.72 (1.34–2.01)
	Late century	0.77 (0.63–1.00)	01/09 (12/23–01/20)	01/12 (12/26–01/23)	1.48 (1.26–1.87)

Relative to the baseline period (1986–2005), cold waves over Central China are projected to occur less frequently and with reduced intensity in both mid- and late 21st century under all three emission scenarios (Figs. 5 and 6). In the mid-century, cold-wave frequency is projected to decrease over most of the study region under all three scenarios, with pronounced spatial heterogeneity (Fig. 5). Under RCP2.6, cold-wave frequency increases of 0.2–0.4 events (locally 0.4–0.6 events) are projected for central-eastern Henan and eastern Hubei, while widespread decreases of − 0.7 to − 0.3 events occur elsewhere, reaching − 1.0 to − 0.7 events in parts of central-southern Henan (Fig. 5a). The extreme minimum temperature decreases slightly (− 1.9 to 0°C) in northeastern Henan but increases by 0.0–2.0°C in other remaining area, with stronger warming (4.0–6.0°C) in southeastern Hunan (Fig. 5d). Under RCP4.5, cold-

wave frequency increases by 0.2–0.4 events in southeastern Henan, central-eastern Hubei, and northeastern Hunan, whereas the remaining regions are projected to experience modest decreases (− 0.3 to 0 events) (Fig. 5b). Extreme minimum temperatures exhibit spatially heterogeneous warming. Most of Henan and Hubei are expected to experience warming of 2.0–4.0°C, exceeding 6.0°C in some eastern regions. In contrast, much of Hunan undergoes slight cooling (− 0.9 to 0°C) (Fig. 5e). Under RCP8.5, the spatial pattern of extreme minimum temperature changes resembles that under RCP2.6, but the areas experiencing a decrease in the frequency are more extensive (− 0.7 to − 0.3 events across most areas), with only a negligible increase (0–0.2 events) in northeastern Hubei (Figs. 5c and 5f).

In the late 21st century, the decrease in cold-wave frequency becomes more pronounced and spatially extensive, whereas changes in extreme minimum temperatures exhibit substantial divergence across scenarios (Fig. 6). Under RCP2.6, the area with decreased cold-wave frequency expands northward, while the area with increased frequency in the central part contracts (Fig. 6a). The area of decreasing in extreme minimum temperatures expands beyond its mid-century extent over northeastern Henan, additionally covering northern Henan, central-eastern Hubei, and central-northern Hunan (Fig. 6d). Under RCP4.5, areas with increased cold-wave frequency contract sharply, remaining only as isolated patches in southeastern Hubei (0–0.2 events). Most regions experience frequency decreases of − 0.8 to − 0.3 events, with local decreases reaching − 1.1 to − 0.8 events in southern Hunan (Fig. 6b). Extreme minimum temperatures exhibit pronounced warming across all sub-regions (Fig. 6e). The most drastic changes are projected under RCP8.5, with widespread and consistent decreases in cold-wave frequency. Reductions of − 1.4 to − 0.8 events are projected in south-central Hunan and northwestern Henan (Fig. 6c). Extreme minimum temperatures increase markedly, exceeding 12.4°C in eastern Henan and northern Hubei. Much of Hunan experience intense warming, whereas localized cooling persists in southern Hubei (Fig. 6f). Overall, these results highlight the enhanced spatial heterogeneity and greater climate instability associated with high-emission pathways.

5 Conclusions and Discussion

Based on a combined dynamical–statistical downscaling dataset at a 6.25-km-resolution and observations from national meteorological stations, this study systematically evaluated the ability of a multi-model ensemble to simulate the present climate over Central China and projected future changes in high-impact climate events. The main conclusions are as follows.

The multi-model ensemble reasonably reproduces the large-scale spatial patterns of mean, maximum, and minimum temperatures over Central China, which are characterized by higher values over southern and over plain areas and lower values over northern and mountainous areas. However, the simulations exhibit a general cold bias in all three temperature variables, with the bias being largest in maximum temperature.

Regional persistent heat events over Central China are projected to become more frequent, more intense, and longer-lasting, as reflected in increased annual frequency, prolonged mean and maximum duration,

higher extreme maximum temperatures during the events, and an expanded affected area. These changes are projected to be more pronounced in the late century under the high-emission scenario (RCP8.5), with the longest-lasting event extending beyond two weeks in regions from eastern Hubei to central Hunan. The central and eastern parts of Central China emerge as the core regions of intensified heat events.

Cold waves over Central China are generally projected to become less frequent and weaker, as evidenced by lower annual frequency, substantially earlier earliest-start and latest-end dates, and shorter duration of individual events. In the late 21st century under the high-emission scenario, cold-wave frequency is projected to decrease by 0.8–1.4 events per year in south-central Hunan and northwestern Henan, while extreme minimum temperatures are projected to rise markedly, with increases exceeding 12.4°C in eastern Henan and northern Hubei.

These findings are consistent with the general understanding, on both global and regional scales, that persistent heat events are becoming more frequent while cold events are decreasing. The high-resolution simulations reveal finer-scale spatial details, such as identifying the central and eastern parts of Central China as a hotspot of heat-event change, which has important implications for regional disaster prevention and preparedness planning. The results also highlight the key role of emission pathways in shaping future climate risks. Under the stringent mitigation pathway (RCP2.6), both the magnitude of temperature increase and the intensification of heat events are generally weaker than under RCP4.5 and RCP8.5. In contrast, under the high-emission pathway (RCP8.5), heat events become extremely frequent, intense, and prolonged, while cold waves become less frequent but still occur.

Future research could further integrate population and socio-economic data to perform dynamic, quantitative risk assessments based on high-resolution climate projection, thereby providing direct and actionable support for fine-scale climate adaptation planning. It should be noted that, however, these projections are conditioned on three CMIP5-driven members, a single regional climate model, and a common statistical downscaling framework, and therefore do not sample the full uncertainty range in future regional climate.

Declarations

Funding: This study was jointly supported by the National Key R&D Program of China (No.2024YFF0809202), the Innovation and Development Project of the China Meteorological Administration (No. CXFZ2026J045) and the Key Innovation Team of National Climate Centre “Third Pole Climate Change Monitoring and Projection” (No. NCCCXTD007).

Conflicts of Interest: The authors declare no conflict of interest.

Data availability: The 6.25-km dynamical–statistical downscaling (HDM) dataset used in this study was developed by Han et al. (2019). The observational data from 299 meteorological stations across Central

China (2008 to 2017) were provided by the National Meteorological Information Centre of China upon reasonable request.

Author contributions: Miao Wang: conceptualization, methodology, formal analysis, writing—original draft. Ying Shi: supervision, funding acquisition, writing—review and editing. Siyan Dong: data curation, validation. Yuping Yan: investigation, visualization. Xiaocong Liu: resources, writing—review and editing.

References

1. Ai YX, Sun JQ, Han ST et al (2020) Spatial and temporal features of spring extreme low temperature events in China during 1961–2016. Chin J Atmos Sci 44(6):1305–1319
2. Ding T, Yuan Y, Zhang J et al (2019) 2018: the hottest summer in China and possible causes. J Meteorol Res 33(4):577–592. https://doi.org/10.1007/s13351-019-8035-5
3. Ding YH (2008) The unprecedented freezing disaster in January 2008 in southern China and its possible association with the globe warming. Acta Meteorol Sin 22:538–558
4. Easterling DR, Evans JL, Groisman PY et al (2000) Observed variability and trends in extreme climate events: a brief review. Bull Am Meteorol Soc 81(3):417–426. https://doi.org/10.1175/1520-0477(2000)081%3C0417:OVATIE%3E2.3.CO;2
5. Fischer EM, Knutti R (2015) Anthropogenic contribution to global occurrence of heavy-precipitation and high-temperature extremes. Nat Clim Chang 5(6):560–564. https://doi.org/10.1038/nclimate2659
6. Fuentes-Franco R, Coppola E, Giorgi F et al (2014) Assessment of RegCM4 simulated inter-annual variability and daily-scale statistics of temperature and precipitation over Mexico. Clim Dyn 42(3):629–647. https://doi.org/10.1007/s00382-013-1885-7
7. Gao XJ, Wu J, Shi Y et al (2018) Future changes in thermal comfort conditions over China based on multi-RegCM4 simulations. Atmos Ocean Sci Lett 11(4):291–299. https://doi.org/10.1080/16742834.2018.1462244
8. Gasparrini A, Guo Y, Hashizume M et al (2015) Mortality risk attributable to high and low ambient temperature: a multicountry observational study. Lancet 386(9991):369–375. https://doi.org/10.1016/S0140-6736(15)60528-6
9. GB/T 21987 – 2017 (2017) Grades of cold wave. China Meteorological Administration. Standardization Administration of China, Beijing, China
10. Giorgi F (2019) Climate change hot-spots. Geophys Res Lett 46(11):6146–6156. https://doi.org/10.1029/2019GL082946
11. Gong Z, Wang X, Cui D et al (2012) The identification and changing characteristics of regional low temperature extreme events. J Appl Meteorol Sci 23(2):195–204. https://doi.org/10.3969/j.issn.1001-7313.2012.02.009
12. Guan Y, Zhang X, Zheng F et al (2015) Trends and variability of daily temperature extremes during 1960–2012 in the Yangtze River Basin, China. Glob Planet Change 124:79–94.

https://doi.org/10.1016/j.gloplacha.2014.12.006

13. Guo C, Zhu XJ, Sun S et al (2023) Analysis of high-temperature hazard in different climatic regions of China. J Trop Meteorol 39(1):66–77. https://doi.org/10.16032/j.issn.1004-4965.2023.005
14. Han Z, Shi Y, Wu J (2019) Combined dynamical and statistical downscaling for high-resolution projections of multiple climate variables in the Beijing–Tianjin–Hebei region of China. J Appl Meteorol Climatol 58(10):2287–2305. https://doi.org/10.1175/JAMC-D-19-0048.1
15. Hasegawa T, Sakurai G, Fujimori S et al (2021) Extreme climate events increase risk of global food insecurity and adaptation needs. Nat Food 2(8):587–595. https://doi.org/10.1038/s43016-021-00356-5
16. Hsu PC, Qian Y, Liu Y et al (2020) Role of abnormally enhanced MJO over the Western Pacific in the formation and subseasonal predictability of the record-breaking Northeast Asian heatwave in the summer of 2018. J Clim 33(8):3333–3349. https://doi.org/10.1175/JCLI-D-19-0749.1
17. Hu S, Zhou T, Peng D et al (2024) Extreme dry advection dominates the record-breaking Yangtze River heatwave in midsummer of 2022. Clim Dyn 62:5049–5060. https://doi.org/10.1007/s00382-024-07150-0
18. IPCC (2021) Climate Change 2021: The Physical Science Basis. Contribution of Working Group I to the Sixth Assessment Report of the Intergovernmental Panel on Climate Change. Cambridge University Press, Cambridge, p 2391. https://doi.org/10.1017/9781009157896
19. James DG, David JF, Upmanu L et al (2021) How unprecedented was the February 2021 Texas cold snap? Environ Res Lett 16(6):064056. https://doi.org/10.1088/1748-9326/abf243
20. Jiang C, Mu X, Wang F et al (2016) Analysis of extreme temperature events in the Qinling Mountains and surrounding area during 1960–2012. Quat Int 392:155–167. https://doi.org/10.1016/j.quaint.2015.12.042
21. Lesk C, Rowhani P, Ramankutty N (2016) Influence of extreme weather disasters on global crop production. Nature 529(7584):84–87. https://doi.org/10.1038/nature16467
22. Li Y, Zhao J, Miao R et al (2022) Analysis of the temporal and spatial distribution of extreme climate indices in central China. Sustainability 14(4):2329. https://doi.org/10.3390/su14042329
23. Li R, Han Z, Xu Y et al (2023) An Ensemble projection of extreme climate events and related risk exposures in the 21st century in the Yangtze River Economic Zone using high-resolution (6.25 km) downscaling datasets. Clim Environ Res 28(1):45–60. https://doi.org/10.3878/j.issn.1006-9585.2022.21140
24. Liu M, Wang K, Wan SQ et al (2020) Central China regional climate change assessment report, 3rd edn. China Meteorological, Beijing, pp 27–33
25. Lou W, Yao Y, Sun K et al (2019) Variability of heat waves and recurrence probability of the severe 2003 and 2013 heat waves in Zhejiang Province, southeast China. Clim Res 79(1):63–75. https://doi.org/10.3354/cr01594
26. Ma S, Zhu C (2019) Extreme cold wave over East Asia in January 2016: A possible response to the larger internal atmospheric variability induced by Arctic warming. J Clim 32(4):1203–1216.

https://doi.org/10.1175/JCLI-D-18-0234.1

27. Mao Y, Li P, Chen X et al (2026) Climate change projections in Central Asia based on the CORDEX-CA-II high-resolution simulations. Atmos Ocean Sci Lett 19(2):100660. https://doi.org/10.1016/j.aosl.2025.100660
28. Maraun D (2016) Bias correcting climate change simulations - a critical review. Curr Clim Change Rep 2(4):211–220. https://doi.org/10.1007/s40641-016-0069-1
29. Meehl GA, Tebaldi C (2004) More intense, more frequent, and longer lasting heat waves in the 21st century. Science 305(5686):994–997. https://doi.org/10.1126/science.1098787
30. Niu X, Tang J, Chen D et al (2021) The performance of CORDEX-EA-II simulations in simulating seasonal temperature and elevation-dependent warming over the Tibetan Plateau. Clim Dyn 57:1135–1153. https://doi.org/10.1007/s00382-021-05760-6
31. Qian C, Zhang X, Li Z (2019) Linear trends in temperature extremes in China, with an emphasis on non-Gaussian and serially dependent characteristics. Clim Dyn 53(1):533–550. https://doi.org/10.1007/s00382-019-04694-0
32. QX/T 228–2014 (2014) Classification of regional high temperature weather process. China Meteorological Administration, Beijing, China
33. QX/T 393–2017 (2017) Monitoring indices of cold air processes. China Meteorological Administration, Beijing, China
34. Robine J-M, Cheung SLK, Le Roy S et al (2008) Death toll exceeded 70,000 in Europe during the summer of 2003. C R Biol 331(2):171–178. https://doi.org/10.1016/j.crvi.2007.12.001
35. Sheffield J, Barrett AP, Colle B et al (2013) North American Climate in CMIP5 Experiments. Part I: Evaluation of Historical Simulations of Continental and Regional Climatology. J Clim 26(23):9209–9245. https://doi.org/10.1175/JCLI-D-12-00595.1
36. Shi Y, Wang G, Gao X (2018) Role of resolution in regional climate change projections over China. Clim Dyn 51(5–6):2375–2396. https://doi.org/10.1007/s00382-018-4252-8
37. Sun W, Mu X, Song X et al (2016) Changes in extreme temperature and precipitation events in the Loess Plateau (China) during 1960–2013 under global warming. Atmos Res 168:33–48. https://doi.org/10.1016/j.atmosres.2015.11.010
38. Sun Y, Zhang X, Zwiers FW et al (2014) Rapid increase in the risk of extreme summer heat in Eastern China. Nat Clim Chang 4(12):1082–1085. https://doi.org/10.1038/nclimate2470
39. Wang H, Pan Y, Chen Y et al (2017a) Linear trend and abrupt changes of climate indices in the arid region of northwestern China. Atmos Res 196:108–118. https://doi.org/10.1016/j.atmosres.2017.07.015
40. Wang M, Liu M, Ren Y et al (2021) Projection of climate change over Central China by high-resolution simulation data under RCP4.5 scenario. J Meteorol Environ 37(3):65–72
41. Wang M, Qin P, She C et al (2023) Simulation and projection of climate change in Central China based on CMIP6 multi-model ensemble. J Meteorol Environ 39(6):51–60

42. Wang Y, Zhou B, Qin D et al (2017b) Changes in mean and extreme temperature and precipitation over the arid region of northwestern China: Observation and projection. Adv Atmos Sci 34(3):289–305. https://doi.org/10.1007/s00376-016-6159-5
43. Wu X, Xu Y, Chen H (2020) Study on the spatial pattern of an extreme heat event by remote sensing: A case study of the 2013 extreme heat event in the Yangtze River Delta, China. Sustainability 12(11):4415. https://doi.org/10.3390/su12114415
44. Yang P, Tang J, Lu Y et al (2025) Evaluation of Very High-Resolution Regional Climate Downscaling over CORDEX East Asia: Climatology and Interannual Variability. J Meteorol Res 39:1228–1246. https://doi.org/10.1007/s13351-025-4249-4
45. Yu Z, Li X (2015) Recent trends in daily temperature extremes over northeastern China (1960–2011). Quat Int 380:35–48. https://doi.org/10.1016/j.quaint.2015.06.042
46. Zhang X, Fu Y, Han Z et al (2022a) Extreme cold events from East Asia to North America in winter 2020/21: Comparisons, causes, and future implications. Springer Clim Springer. https://doi.org/10.1007/978-3-030-98089-7
47. Zhang Y, Fu L, Pan J et al (2017) Projected changes in temperature extremes in China using PRECIS. Atmosphere 8(1):15. https://doi.org/10.3390/atmos8010015
48. Zhang Y, Sun S, Liu Y et al (2022b) Global major weather and climate events in 2021 and possible causes. Meteorol Mon 48:459–469. https://doi.org/10.11898/1001-7313.2022046
49. Zhou T, Zhang W, Zhang L 2021: a year of unprecedented climate extremes in Eastern Asia, North America, and Europe. In: Springer Climate., Springer et al (2022) https://doi.org/10.1007/978-3-031-08169-3
50. Zscheischler J, Westra S, Van Den Hurk BJ et al (2018) Future climate risk from compound events. Nat Clim Chang 8(6):469–477. https://doi.org/10.1038/s41558-018-0199-1

Figures

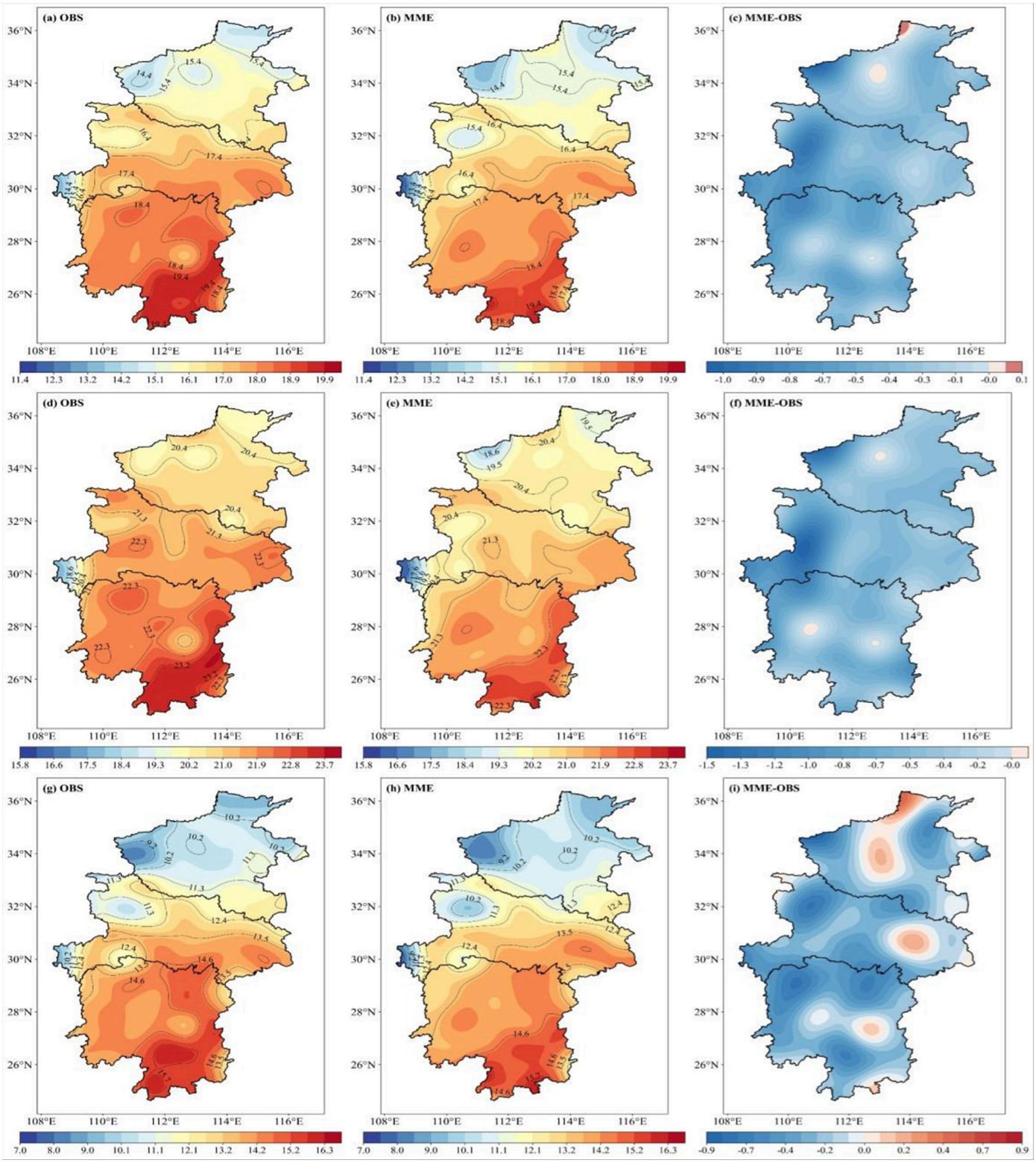


Figure 1

(a, d, g) Observed, (b, e, h) simulated and (c, f, i) model bias of annual (a–c) mean temperature, (d–f) maximum temperature, and (g–i) minimum temperature over Central China during 2008–2017

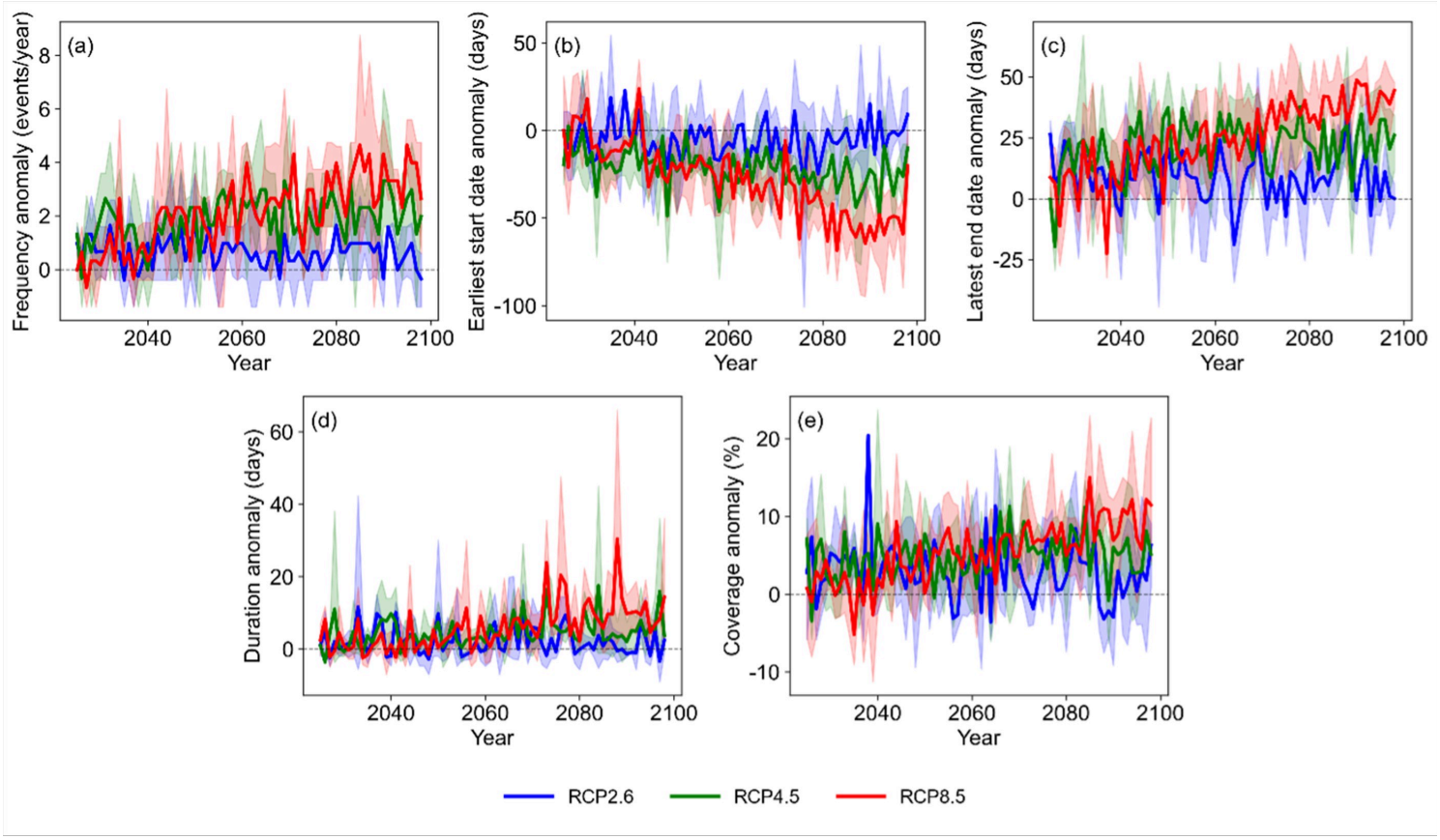


Figure 2

Projected changes in regional persistent heat events averaged over Central China under RCP2.6, RCP4.5, and RCP8.5, expressed as anomalies relative to the 1986–2005 baseline: annual mean (a) frequency, (b) earliest start date, (c) latest end date, (d) event duration, (e) coverage area with maximum temperature ≥ 35°C

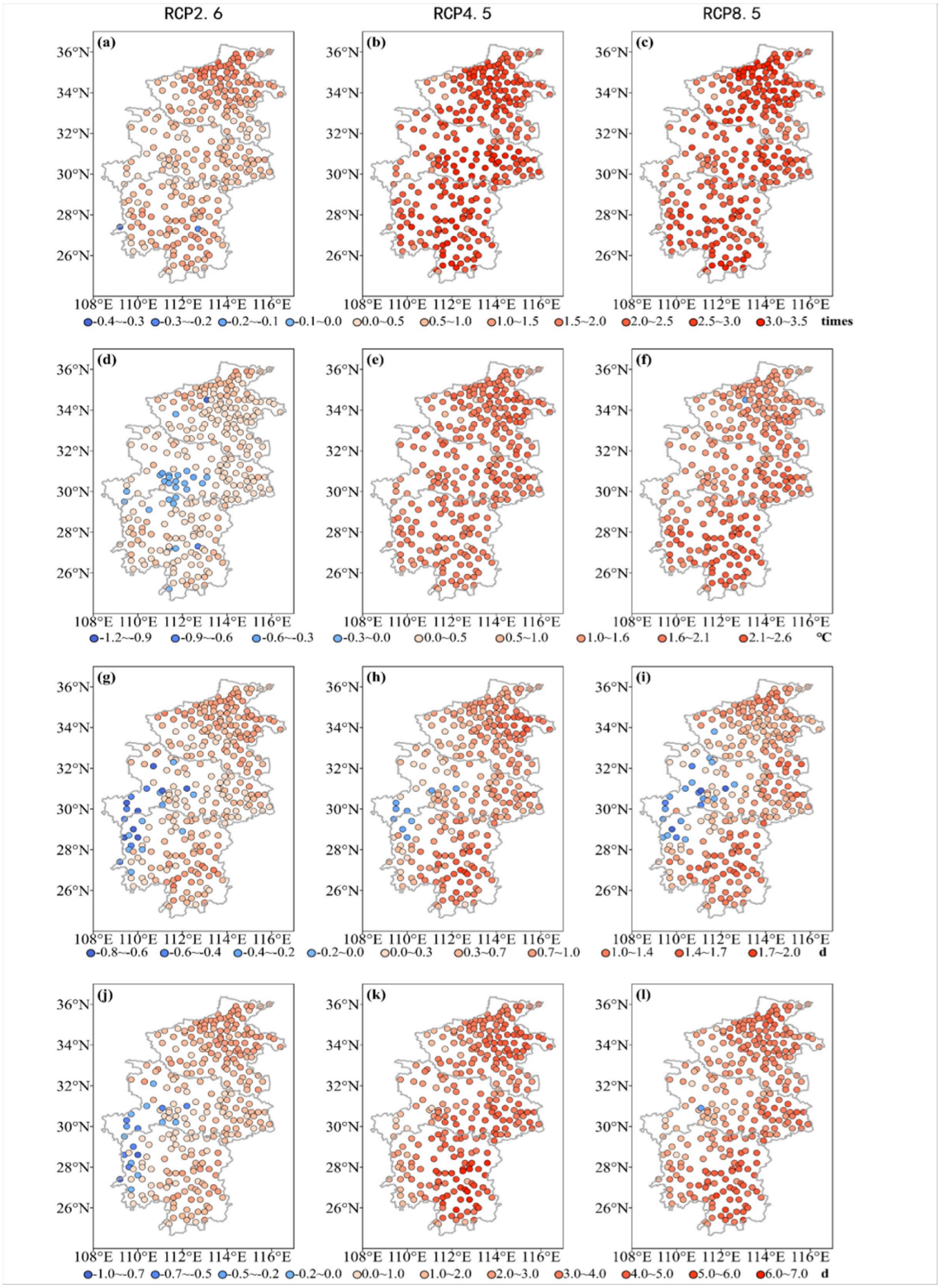


Figure 3

Changes in single-station persistent heat events over Central China in the mid-21st century under the RCP2.6 (a, d, g, j), RCP4.5 (b, e, h, k), and RCP8.5 (c, f, i, l) scenarios relative to the 1986–2005 baseline period: (a–c) frequency, (d–f) extreme maximum temperature, (g–i) mean duration and (j–l) maximum duration

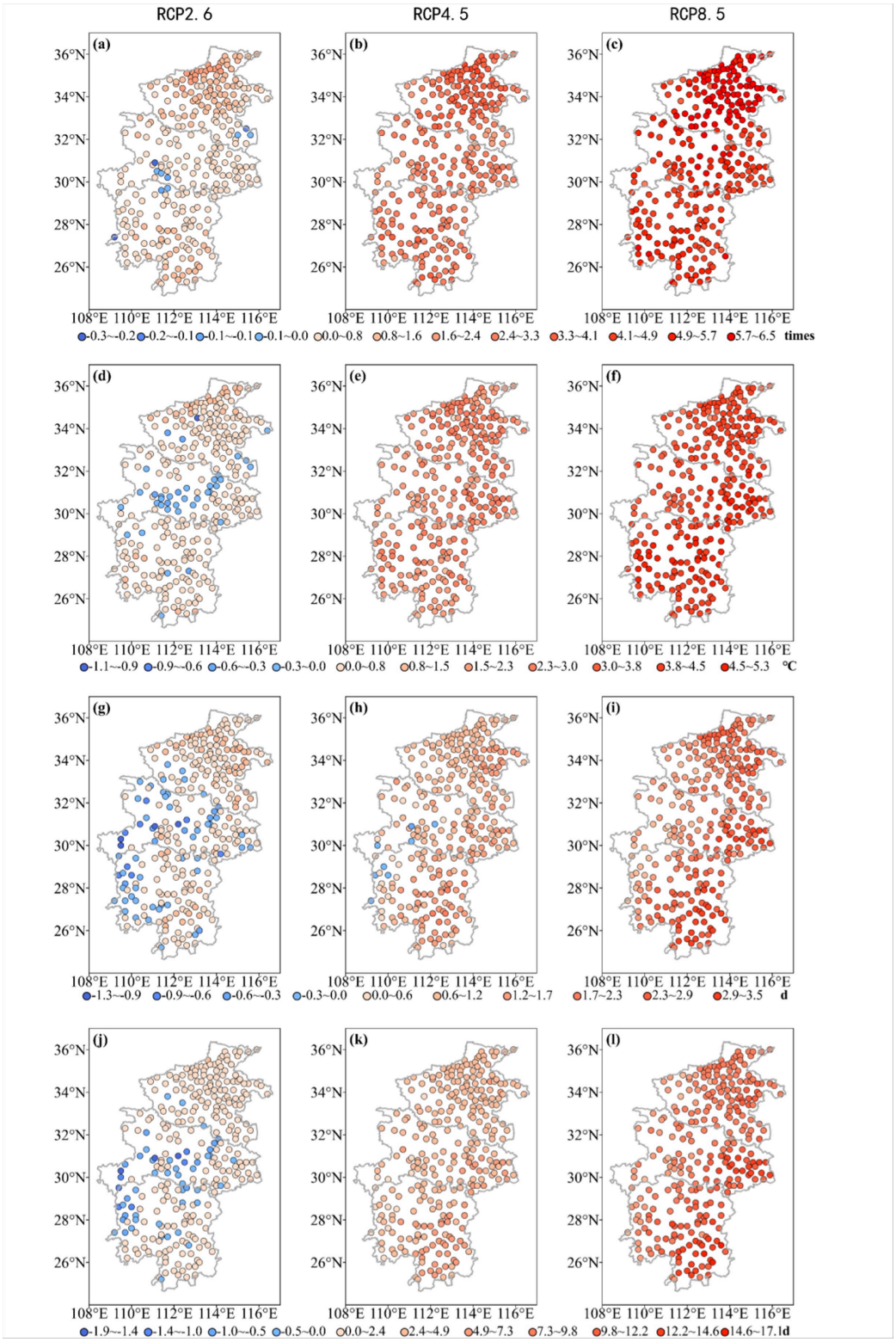


Figure 4

Same as Fig. 3, but for the late 21st century

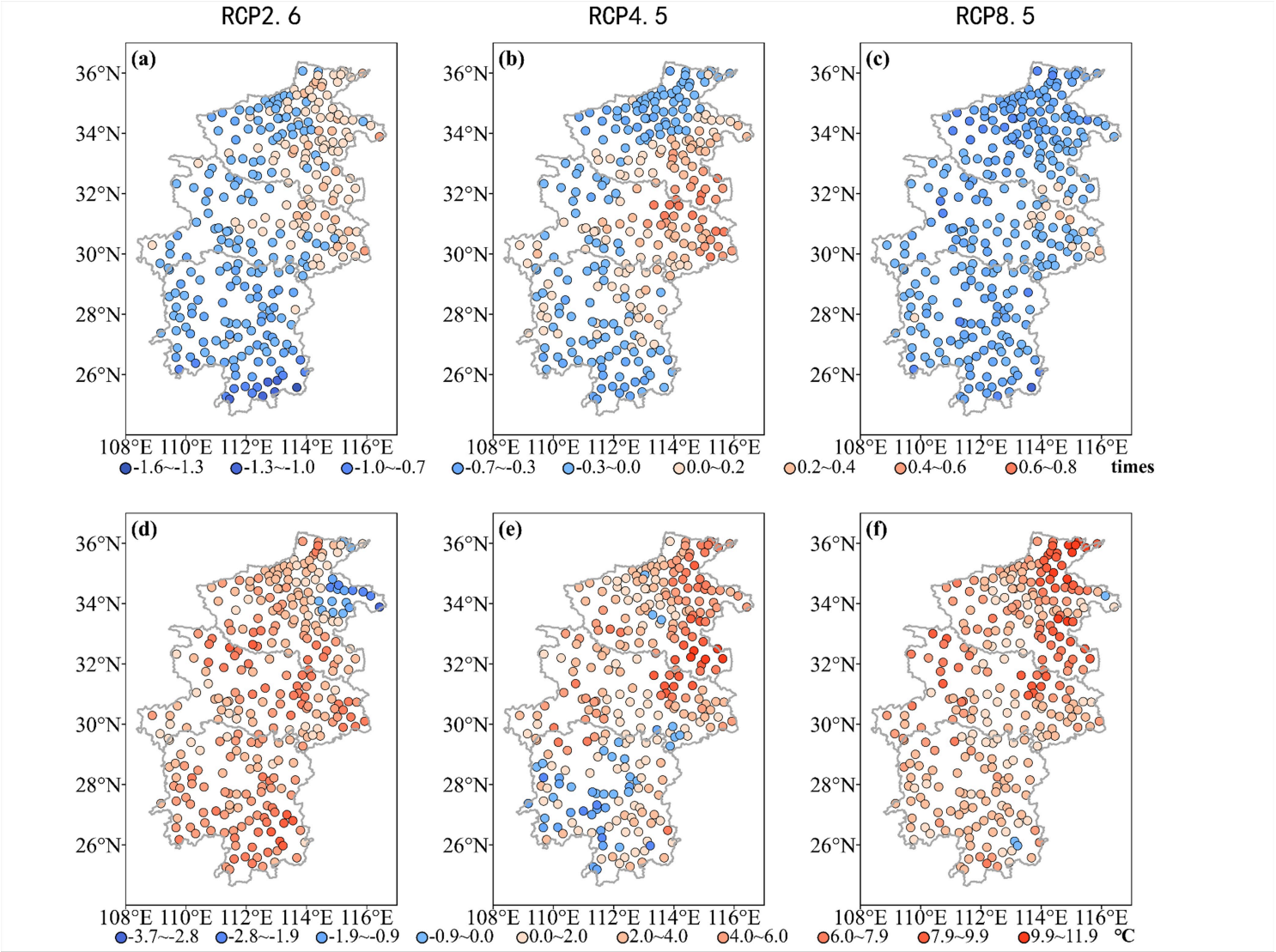


Figure 5

Changes in cold waves over Central China in the mid-21st century under the (a, d) RCP2.6, (b, e) RCP4.5, and (c, f) RCP8.5 scenarios relative to the 1986–2005 baseline period: (a–c) frequency, (d–f) extreme daily minimum temperature

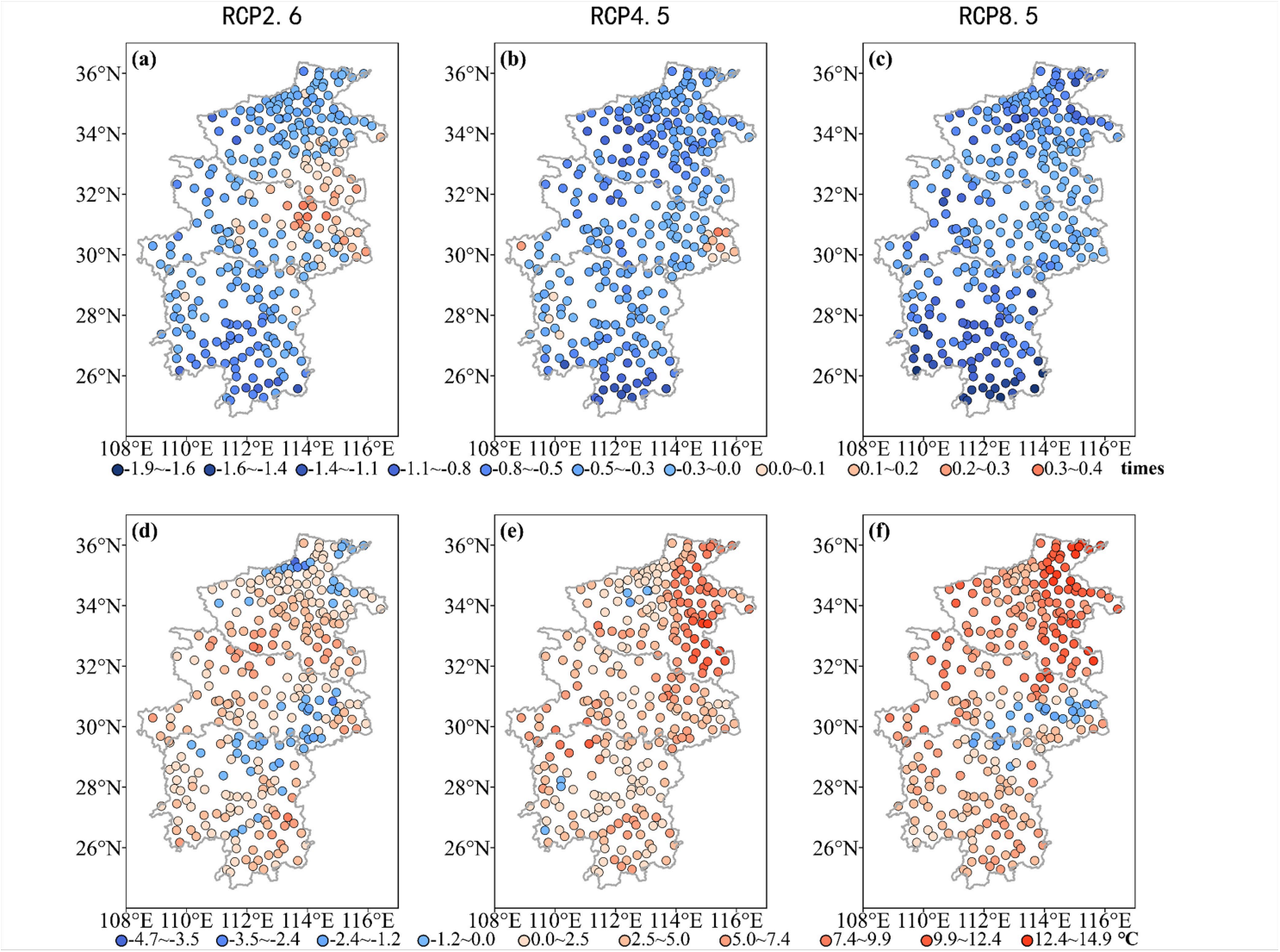


Figure 6

Same as Fig. 5, but for the late 21st century